Interactions Between Nucleic Acid Ions and Electrons and Photons

4

Steen Brøndsted Nielsen

Abstract

This chapter deals with nucleic acid ions and their interactions with electrons and photons in the gas phase based on the many different experiments that have been performed relating to this topic within the last 10 years. The fragmentation caused by electron attachment to anions is discussed, and the role of hydration is touched upon. Photoelectron spectroscopy has established the electron binding energies of mononucleotide anions, dinucleotides and larger strands. These are significantly lower than the thresholds for electron-induced electron detachment from anions. Thresholds were measured from electron scattering experiments and product ion masses from mass spectrometry. The site of electron removal is either the base or the phosphate group, and it is likely different for photodetachment and electron detachment. Work has not been limited to anions only, but cations have also been studied. Neutral reionisation of protonated nucleobases has shed light on the lifetime of the neutral intermediate species, which was found to be significantly different to that of the temporary nucleobase anion formed in collisional electron transfer to nucleotide anions. Dissociative recombination experiments involving oligonucleotide monocations have demonstrated that there are certain electron kinetic energies where the cross section for the formation of neutral species is high (resonances), and in closely related electron-capture dissociation experiments on multiply charged cations, the actual fragmentation channels were obtained. Both for oligonucleotide anions and cations, formation of radicals by loss and capture of electrons, respectively, largely governs the dissociation patterns. This is of high relevance for sequencing. Finally, gas-phase absorption spectroscopy has revealed differences in absorption between mononucleotides, single strands, double strands and quadruplexes, which is related to the electronic coupling between two or more bases.

S. Brøndsted Nielsen (✉)
Department of Physics and Astronomy, Aarhus University, 8000 Aarhus C, Denmark
e-mail: sbn@phys.au.dk

V. Gabelica (ed.), *Nucleic Acids in the Gas Phase*, Physical Chemistry in Action,
DOI 10.1007/978-3-642-54842-0_4,

Keywords
Storage ring experiments • Absorption spectroscopy • Photoelectron spectroscopy • Electron detachment • Transient species • Repulsive Coulomb barrier • Nucleobase dehydrogenation

Abbreviations

DEA	Dissociative electron attachment
DR	Dissociative recombination
DSB	Double strand break
ECD	Electron capture dissociation
EDD	Electron detachment dissociation
EPD	Electron photodetachment dissociation
ETD	Electron transfer dissociation
FTICR	Fourier transform ion cyclotron resonance
HOMO	Highest occupied molecular orbital
IC	Internal conversion
SSB	Single strand break
UV	Ultraviolet
VDE	Vertical detachment energy

4.1 Introduction

Ultraviolet (UV) light or ionising radiation can be hazardous for living organisms, either directly or indirectly. Nucleic acids strongly absorb UV light in the UVC range of the solar spectrum (<290 nm) with a maximum at 260 nm, the excitation being a direct $\pi\pi^*$ transition in the base [1–3]. However, they are surprisingly photostable except for the formation of cyclobutane pyrimidine dimers [4–6] that can lead to cancer if not enzymatically repaired. Photoexcited single bases rapidly convert electronic energy into harmless heat which may have been important for their evolutionary selection as the carriers of genetic information [7–9]. Photodissociation of isolated mononucleotide ions in vacuo occurs on the microsecond timescale [10] and can therefore not compete with vibrational cooling in water (few picoseconds) [7]. The situation is, however, more complicated and less understood for strands due to electronic coupling between two or more bases in the excited state [7–9, 11–13]. Indeed, the quantum dynamics for photoexcited strands is up for much current debate, with the role of charge-transfer states and their lifetimes being particularly unclear. It is an open question whether DNA affords self-protection against UV light.

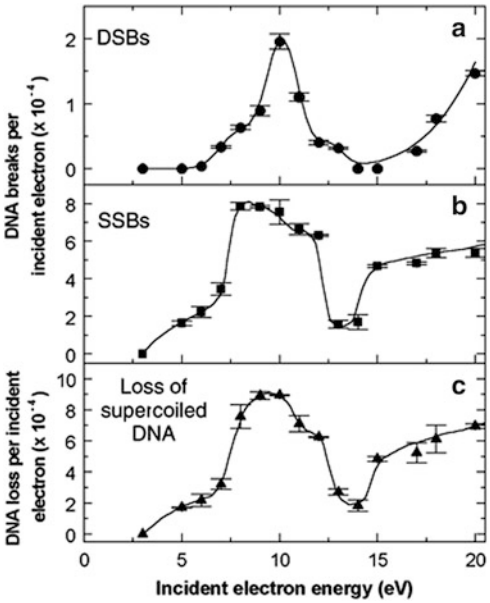

Fig. 4.1 Quantum yields per incident electron for the induction of double strand breaks (DSBs) (**a**), single strand breaks (SSBs) (**b**) and the loss of DNA supercoiled form (**c**) in DNA solids by low-energy electrons versus incident electron energy. Taken from [16] [Copyright permission: a prize is asked for]

Another cause of radiation damage is the formation of secondary species by ionisation of, for example, water. Thus, ionising radiation (β-, x- or γ-rays) produces free secondary electrons in living cells with energies between ~1 eV and 20 eV [14, 15] that are able to induce genotoxic damage such as single and double DNA strand breaks. This was first demonstrated by Huels, Sanche and co-workers [16] from exposing plasmid DNA on a surface held under ultrahigh vacuum to an electron beam of variable and well-defined energy (Fig. 4.1). The DNA samples were relatively dry and contained only structural water molecules, and the phosphate groups likely had counter ions or protons closely bound to them (overall the samples were neutral). At energies well below the ionisation threshold, it is evident that the electrons induced substantial damage to the DNA caused by rapid decays of transient molecular resonances localised on the DNA's basic components.

In other work, Sanche and co-workers [17] found that even lower-energy electrons produced single strand breaks (Fig. 4.2) with a sharp peak at 0.8 eV and a broader feature centred at 2.2 eV. The shape of the curve is very similar to those obtained from dissociative electron attachment (DEA) cross section measurements on nucleobases in vacuo reported by several researchers [18–24]. Radiation damage of DNA and RNA seems therefore to originate from attachment of low-energy electrons to nucleobases. The formed radical anions induce chemical reactions that lead to strand breaks. In agreement with this, Simons and co-workers [25–29] concluded based on extensive theoretical calculations that the most likely pathway is electron attachment to base π* orbitals followed by sugar–phosphate C–O σ bond scission as this dissociation process occurs with the lowest barrier height (ca. 0.5

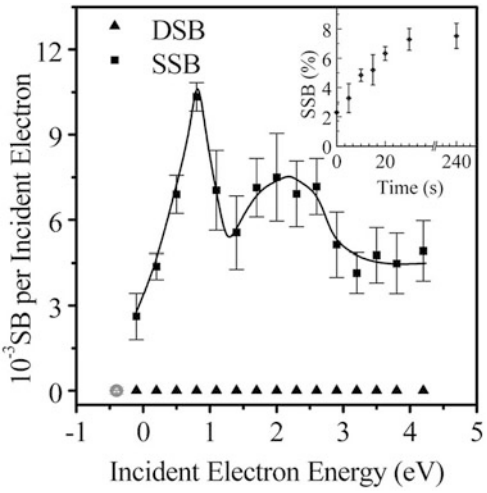

Fig. 4.2 Quantum yield of DNA SSBs and double-strand breaks as a function of incident electron energy. The *inset* shows the percentage of SSBs versus time for 0.6 eV electrons. Taken from [17]. Copyright (2004) by The American Physical Society

eV) compared to those for others (e.g. sugar-base N–C bond breakage). As the C–O bond stretches, the electron promptly moves via a through-bond transfer process from the base π* orbital through the vacant orbitals of the intervening deoxyribose to the C–O σ* orbital [28]. Interestingly, base π-stacking was found to increase the barrier thereby lowering the rate of SSBs [26]. Both the theoretical and experimental data relate to neutral samples in which there are no negative charges from ionised phosphate groups. Taken together, the studies nicely demonstrated how the interpretation of results obtained on solid DNA samples was aided by results from gas-phase experiments and theory on simple model systems.

A full understanding of the interactions between nucleic acids and light or electrons is nontrivial because of the large complexity of DNA and the complicating role of the nearby environment (water molecules or counter ions). A reductionist approach has therefore been taken by many and resulted in studies on small DNA building blocks such as single bases (as mentioned above), mononucleotides or smaller oligonucleotides isolated in vacuo. In this chapter results from such experiments will be presented, and the focus is on charged species that can easily be made by electrospray ionisation (see Chap. 2) and investigated by mass spectrometry techniques. While a connection or importance of many of the results to "real" biology is still to emerge, they are of immediate relevance for the determination of the sequence of bases in oligonucleotides, are of fundamental interest to physical chemists and are used to benchmark theoretical calculations. The hope is that isolated strands in vacuo will serve as good models to bridge the gap between gas-phase studies of single bases and solution-phase studies on DNA.

This chapter is organised in the following way: First, results on electron attachment to nucleotide ions (both anions and cations) are presented. This section is followed by a description of electron scattering and electron detachment experiments on negative ions. Next photoelectron spectroscopy and absorption spectroscopy on negative ions are discussed. Finally, the status of the results

obtained so far is given. It should be said that the chapter focuses more on electron interactions than on light interactions, which will be covered by Chap. 5 in this volume and in another volume in the same series (by J.M. Weber, J. Marcum and S. Brøndsted Nielsen) dedicated to spectroscopy of the nucleic acids in gas phase. Also fragmentation reactions of nucleic acids in gas phase are only briefly discussed here, as they are presented in Chap. 6.

4.2 Electron Attachment to Nucleotide Ions

Experiments have been done for both anions and cations, the former possess one or more negatively charged phosphate groups and neutral bases while the latter have one or more protonated bases and phosphoric acid groups. The two polarity cases are discussed separately.

4.2.1 Anions

The attachment of free electrons to nucleotide anions in vacuo is prevented by the long-range Coulomb repulsion between the two collision partners. It relies on electron tunnelling through the repulsive Coulomb barrier, which occurs with low probability (Fig. 4.3). To circumvent this obstacle, Hvelplund, Brøndsted Nielsen and co-workers [30, 31] instead did high-energy collisions between monoanions and alkali metal atoms, e.g. sodium and caesium. The latter act as electron donors due to their weakly bound *s* electrons. An ion accelerated to 50 keV kinetic energies moves with a velocity of about 10^5 m/s and passes by an atom within a few femtoseconds. In this interaction time, there is a finite probability for electron transfer to occur. The energy levels of the anion are Stark shifted as a result of the electric field of the sodium (or caesium) cation facilitating resonant electron transfer at large impact parameters. The collisional electron transfer process is to a good approximation vertical as the nuclei do not have time to move during the brief encounter. Popularly speaking, the so-formed fast-moving dianion leaves the sodium ion behind before the electron realises that it is unfavourable for it to be on the anion. However, now it is trapped as it has to tunnel out through the repulsive Coulomb barrier, which occurs with low probability, just as for the opposite process discussed earlier for the interaction between the anion and a free electron. A similar more well-known situation is alpha particle decay.

In this way, electron transfer to mononucleotide and larger oligonucleotide anions was successfully done [32]. An example illustrating the product ions produced in collisions between AMP anions (adenosine 5′-monophosphate, i.e. deprotonated AMP molecule) and sodium is shown in Fig. 4.4. For comparison the spectrum obtained with neon as the collision gas is also included in the figure. Neon has a similar geometrical cross section to that of sodium, but its high ionisation energy prevents it from participating in electron transfer; hence, peaks of similar magnitude seen in both the Na and Ne spectra are due to collision-

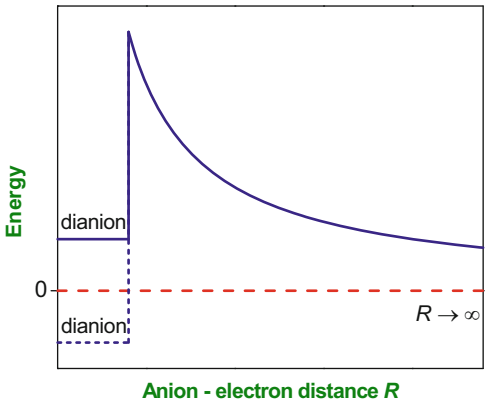

Fig. 4.3 Potential energy between a monoanion and an electron as a function of their separation. At short distances there may be either stable (<0) or unstable (>0) electronic states due to the favourable attraction between the electron and the nuclei. At larger distances, the curve follows Coulomb's law, 14.4 eV Å/R

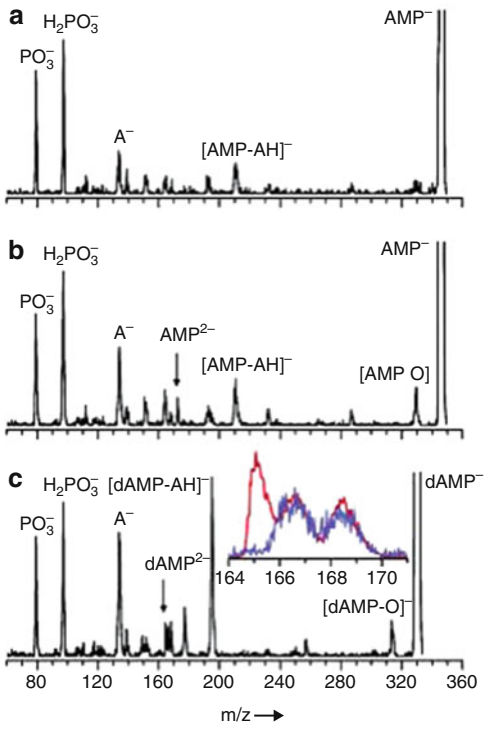

Fig. 4.4 Spectra obtained after high-energy collisions between AMP anions (*m*/*z* 346) and neon (**a**) and sodium (**b**) and between dAMP anions (*m*/*z* 330) and sodium (**c**). The *inset* in (**c**) shows the region around half the *m*/*z* of the dAMP anion for collisions between dAMP anions and neon (*blue curve*) or sodium (*red curve*). Taken from [32]

induced dissociation not involving electron transfer. Evidently, the oxygen loss channel significantly increases in importance from Ne to Na, which is indicative of dissociative electron capture. It is unclear which oxygen is lost, and whether the loss is due to electron attachment to a base π* orbital or to the phosphate P=O π* orbital, though the latter is highly unfavourable due to the Coulomb repulsion from the negative charge.

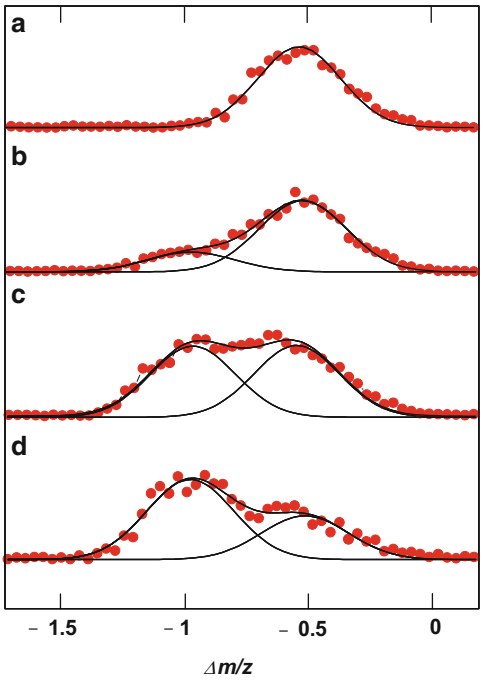

Fig. 4.5 Narrow scan mass spectra in the region of the dianion formed in collisional electron transfer experiments between sodium atoms and AMP anions containing different numbers of deuterium. Zero corresponds to the intact dianion. (a) AMP^-. (b) d_1-AMP^-. (c) d_2-AMP^-. (d) d_3-AMP^-. The more deuterium in the initial monoanion, the larger is the peak corresponding to loss of D compared to loss of H. Reprinted with permission from [33]. Copyright 2004, AIP Publishing LLC

There is a small but discernible sharp peak at about half the m/z of the parent ion, which is only seen in the Na spectrum. A similar result was found for the dAMP mononucleotide (deoxyadenosine 5′-monophosphate) (Fig. 4.4c). These findings indicate that dianions are formed. The extra electron is located in an antibonding covalent orbital on the nucleobase and is predicted to be unbound. Experiments done with higher mass resolution and accuracy show that the dianions are actually dehydrogenated. Hence, electron capture is followed by rapid loss of a hydrogen atom (within the few microsecond travel time to the analyser). Experiments on deuterated ions confirmed this conclusion and revealed that the origin of the hydrogen is a heteroatom (Fig. 4.5) [33], either a nitrogen (NH_2) of the adenine, a sugar oxygen (OH) or a phosphate oxygen (POH). Deuterated ions were formed by dissolving the nucleotide in a solution of D_2O, CD_3OD and CH_3COOD for electrospray ionisation and carefully saturating the region around the electrospray needle with heavy water to prevent back exchange during electrospray. Only hydrogens bound to heteroatoms are exchangeable in such experiments. Loss of hydrogen from the phosphoric acid group seems highly unlikely as doubly deprotonated AMP cannot be made by electrospray ionisation because the Coulomb repulsion between two nearby negatively charged oxygen atoms would be too large. Furthermore, experiments on all eight mononucleotides (AMP, CMP, GMP, UMP, dAMP, dCMP, dGMP, dTMP) revealed strong differences in the cross section for formation of dehydrogenated ions from transient dianions, which indicates that the base plays a key role. Cross sections were determined by varying the pressure of

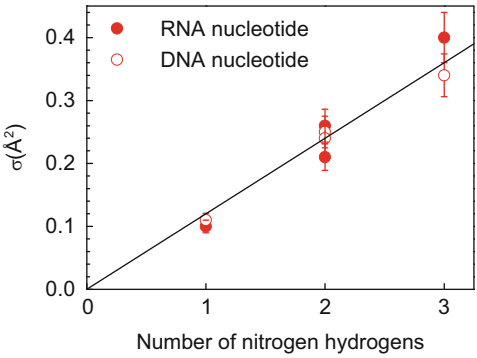

Fig. 4.6 The cross section for formation of dehydrogenated mononucleotide dianions as a function of the number of NH hydrogens (1, 2, or 3). Uracil and thymine (1), cytosine and adenine (2) and guanine (3). Reprinted with permission from [33]. Copyright 2004, AIP Publishing LLC

sodium atoms. A clear linear correlation between the cross section and the number of NH hydrogens in the base was found, and an extrapolation to zero NH hydrogens gave a zero cross section (Fig. 4.6), which is in strong support of the hydrogen loss originating solely from the NH base groups. Thus, nucleotides with thymine or uracil bases have the lowest cross sections while those with guanine have the highest, and nucleotides with cytosine or adenine are in between. Also there is no difference between RNA and DNA nucleotides, which implies that substitution of the OH on C2′ with H is unimportant.

These findings are in full agreement with the work done by Desfrançois, Scheier, Farizon, Märk, Illenberger and co-workers [18–24]. They measured the outcome of resonant attachment of low-energy electrons (0–3 eV) to isolated nucleobases as a function of electron energy and found that electron attachment promptly led to hydrogen loss in addition to the formation of a multitude of small fragment anions. Several resonances were identified. From isotope-labelling studies, it was established that NH was the site of dehydrogenation (Fig. 4.7) [24]. The reaction is driven by the large electron affinity of the dehydrogenated radical. Finally, it is worth mentioning that dissociative electron attachment to deoxyribose leads to dehydrogenation but as a minor channel [34].

Next, the role of hydration on nucleotide anions was considered from collisional electron transfer experiments on nanosolvated AMP anions [35]. Spectra for $AMP^{-}(H_2O)_{10}$ and $AMP^{-}(H_2O)_{16}$ are shown in Fig. 4.8. Peaks that correspond to a distribution of hydrated $[AMP - H]^{2-}$ dianions are clearly seen. In all cases, electron transfer induces loss of hydrogen and loss of some or all of the water molecules. Careful calibration experiments were carried out to confirm that hydrogen loss had indeed occurred. Interestingly, the cross section for formation of dehydrogenated dianions increased with the number of water molecules m in the initial cluster (Fig. 4.9). Hence, the damage of the nucleotide was smallest for the bare nucleotide ($m = 0$) and more than fifty times larger for $m = 16$. This contrasted with high-energy collision-induced dissociation experiments that showed that the intact AMP anion would survive when surrounded by enough water molecules as evaporation of the water molecules would cool the ion [36]. On the other hand, for electron capture the energy of the dianion state is lowered by hydration thereby

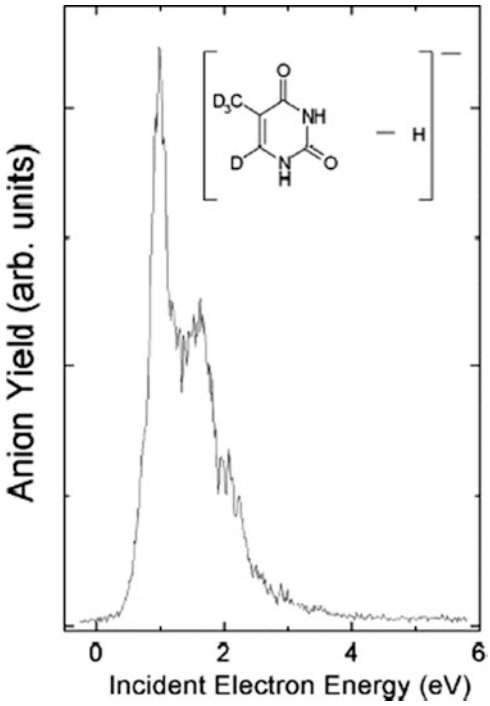

Fig. 4.7 Dissociative electron attachment to deuterium-labelled thymine (C–D) induces selective loss of hydrogen from NH at low electron energies. Taken from [24]. Copyright (2004) by The American Physical Society

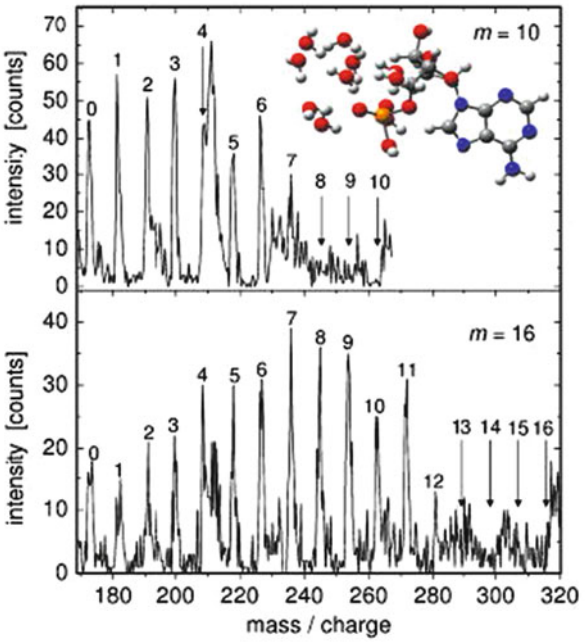

Fig. 4.8 Mass spectra obtained after collisions between sodium atoms and either $AMP^{-}(H_2O)_{10}$ or $AMP^{-}(H_2O)_{16}$. The numbers label the number of water molecules attached to the dehydrogenated dianion, $[AMP - H]^{2-}$. Reprinted with permission from [35]. Copyright 2008, AIP Publishing LLC

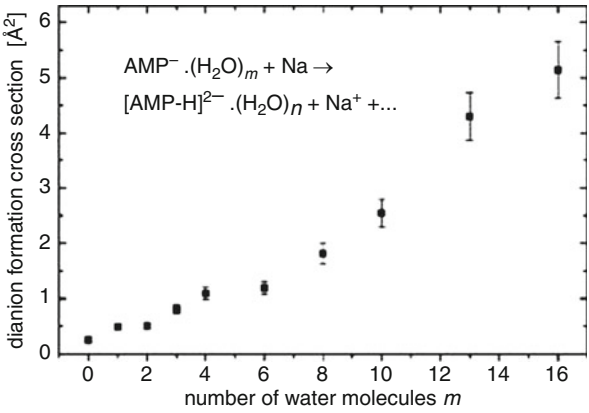

Fig. 4.9 Absolute experimental cross sections for the total formation of dianions as a function of the number of water molecules m attached to the AMP anion. They were obtained by adding the intensities in the $[AMP - H]^{2-}(H_2O)_n$ peaks for $0 \leq n \leq m$. Reprinted with permission from [35]. Copyright 2008, AIP Publishing LLC

lowering the energy defect of the collisional electron transfer process rendering it more likely.

Finally, it is worth to point out that nucleobase anions can be generated by a supersonic expansion nozzle ion source or through electron transfer collisions between the bases and laser-excited Rydberg atoms as demonstrated by Bowen and co-workers [37] and Desfrançois and co-workers [18], respectively. The extra electron is dipole bound by about 0.1 eV or less and is located in a huge and diffuse orbital at the positive end of the molecule's permanent dipole moment. However, as beautifully shown by Bowen and co-workers [38] through photoelectron spectroscopy of the uracil anion, a dipole bound-to-covalent state transformation occurs after just one water molecule is bound to the anion (Fig. 4.10). Dipole-bound anions exhibit a single, strong, narrow feature at very low electron binding energies in contrast to valence anions that give broad bands due to structural differences between the anion and its corresponding neutral. The water molecule stabilises the covalent anion more than the dipole-bound one as the former has a denser excess electron distribution. With xenon attached both dipole-bound and covalent-like features were seen while in the case of argon and krypton only dipole-bound forms are present (Fig. 4.10).

4.2.2 Cations

Collisional electron transfer experiments have also been performed for protonated nucleobases. Since neutrals are produced, reionisation in a second collision is necessary for mass spectrometric detection. This is done after deflection of all ions from the beam by an electric field, cf., neutral reionisation (NR) mass spectrometry. Figure 4.11 shows $^{+}NR^{+}$ spectra obtained by Wyer et al. [39] using caesium and molecular oxygen as electron-donating and electron-stripping gases, respectively, for the five protonated nucleobases. While dehydrogenated cations were clearly observed, intact cations were also measured. It implies that some

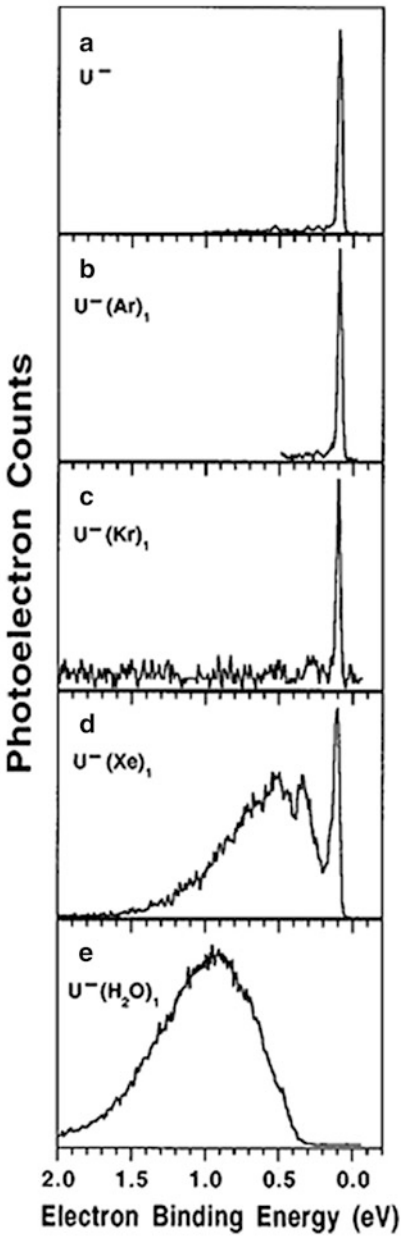

Fig. 4.10 Photoelectron spectra of (**a**) U^-, (**b**) U^-(Ar), (**c**) U^-(Kr), (**d**) U^-(Xe) and (**e**) $U^-(H_2O)$ recorded using 2.540 eV photons. *U* uracil. Reprinted with permission from [38]. Copyright 1998, AIP Publishing LLC

neutralised species survive the 2 μs flight time between the two collision cells. This is in clear contrast to the fact that neutral bases in nucleotides promptly lose hydrogen after electron capture.

Multiply charged oligonucleotide cations have also been subjected to electron capture dissociation (ECD) [40–43] and electron transfer dissociation (ETD) [44]

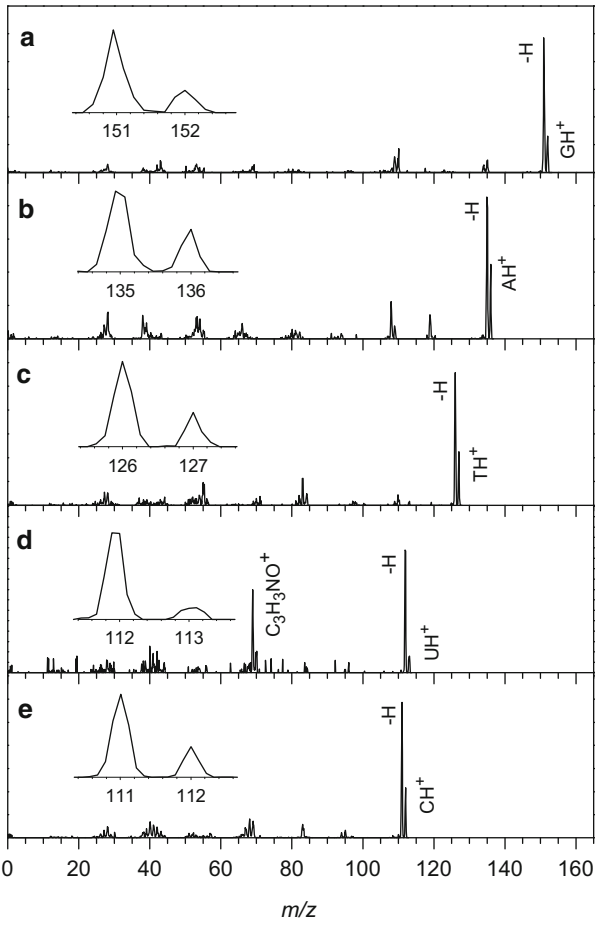

Fig. 4.11 $^{+}NR^{+}$ (i.e. conversion of cations to neutrals and back to cations) spectra resulting from high-energy collisions of MH^{+} with Cs and O_2. (**a**) M = G, (**b**) M = A, (**c**) M = T, (**d**) M = U and (**e**) M = C. Taken from [39]

experiments. The former ions recombine with low-energy electrons in the cell of a Fourier-Transform Ion Cyclotron Resonance (FTICR) instrument while the latter ions react with atomic or molecular anions, often fluoranthene anions, in an ion trap. The preferred site of neutralisation is the protonated nucleobase and not the P=O bonds [43, 45]. Schultz and Håkansson [40] showed that ECD followed by infrared heating caused extensive fragmentation of charge-reduced oligonucleotide cations. Of particular importance cleavage of carbon–oxygen bonds at different sides of an inter-residue phosphate group occurred to produce sequence-specific fragment ions. Likewise, Smith and Brodbelt [44] found that ETD followed by low-energy CID provided better sequence coverage than CID alone and a decrease of base loss and internal fragments. Base loss is a low-energy dissociation channel, and it therefore dominates CID. For large oligonucleotides base loss is rather uninformative and undesired, at least when it comes to establishing the oligonucleotide sequence. Similar experiments on oligonucleotide duplexes resulted in specific backbone

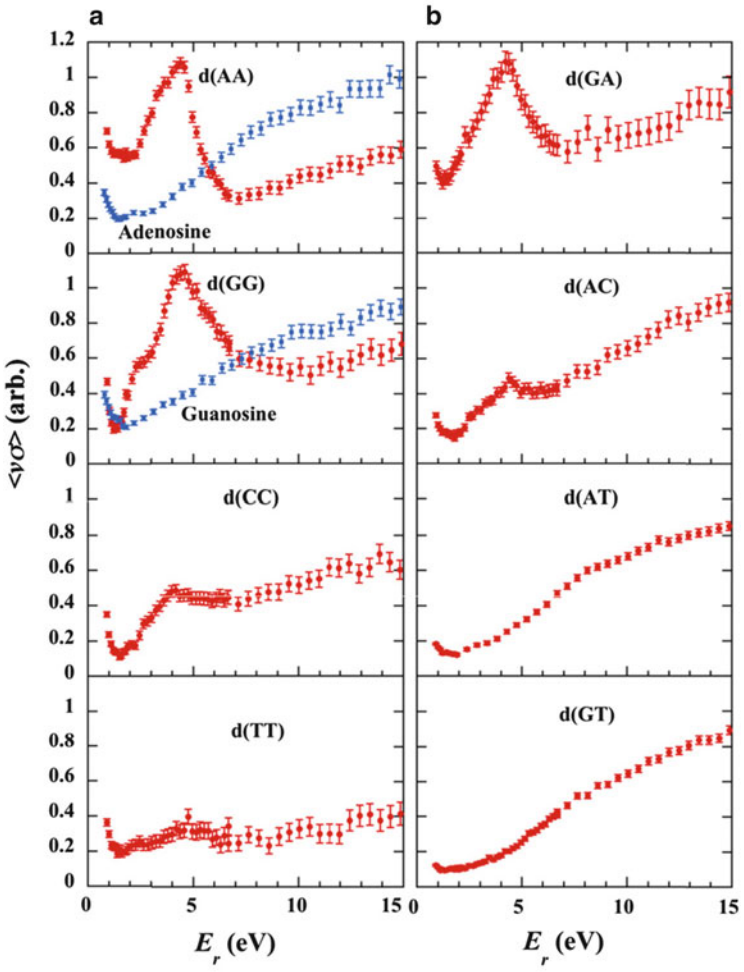

Fig. 4.12 Rates for the formation of neutral species for singly protonated mononucleotides and dinucleotides versus electron energy. Reprinted from [46], Copyright 2006, with permission from Elsevier

cleavages with conservation of weak non-covalent bonds, which is of importance for probing higher-order structures [44].

Finally, Tanabe and co-workers [46] have bombarded mononucleotide and oligonucleotide cations with electrons in an electrostatic ion storage ring (vide infra). Here the rate of formation of neutrals is measured at well-defined electron kinetic energies (Fig. 4.12). The authors found an increased yield in the formation of neutrals at a collision energy of about 4.5 eV in the case of d(A_2), d(G_2), d(C_2), d(GA) and d(AC) DNA dinucleotides and longer strands, and to a lesser extent for d(T_2), whereas no such resonances were observed for mononucleotides and for

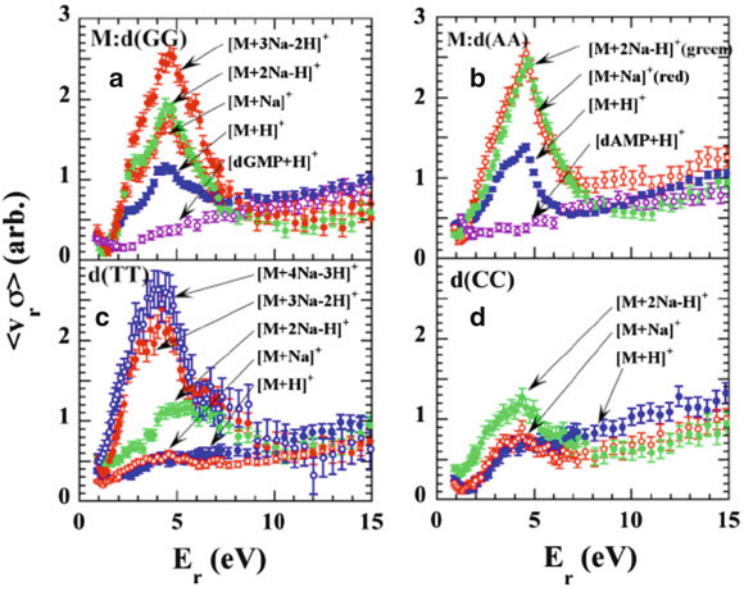

Fig. 4.13 Rates for production of neutral particles in collisions between electrons and $[M + n\,Na - (n–1)\,H]^+$ dinucleotide cations where M is $d(G_2)$ (**a**), $d(A_2)$ (**b**), $d(T_2)$ (**c**) and $d(C_2)$ (**d**). The rates for protonated dGMP and dAMP are also included. Reprinted from [47], Copyright 2008, with permission from Elsevier

dinucleotides containing one thymine base. These results indicate that the incoming electron excites an electronic state at 4.5 eV that involves two stacked bases, i.e. a delocalised state. The electron thereby loses its kinetic energy and gets captured by the cation. Molecular dissociation likely follows (cf., dissociative recombination, DR). These bumps in the production rates of neutrals become even more pronounced when one or more protons are replaced by sodium ions (Fig. 4.13) [47], which is likely ascribed to conformational differences between protonated and sodiated nucleotides.

4.3 Electron Scattering and Detachment Experiments

Mononucleotide and oligonucleotide anions have been subjected to electron scattering experiments using electrostatic ion storage rings that benefit from easy storage of heavy ions. In such experiments, ion bunches are injected into a ring where they circulate due to bending in electrostatic deflectors. In one side of the ring, the ions interact with an electron target, either in crossed beam (ELISA set-up) [48, 49] or in merged beam (KEK set-up) [50, 51] configurations (see Fig. 4.14). The advantage of using a storage ring for these experiments is that the ions move with high velocities so that the relative energy (E_r) between the two collision partners can be finely controlled and varied. Best resolution is obtained in the

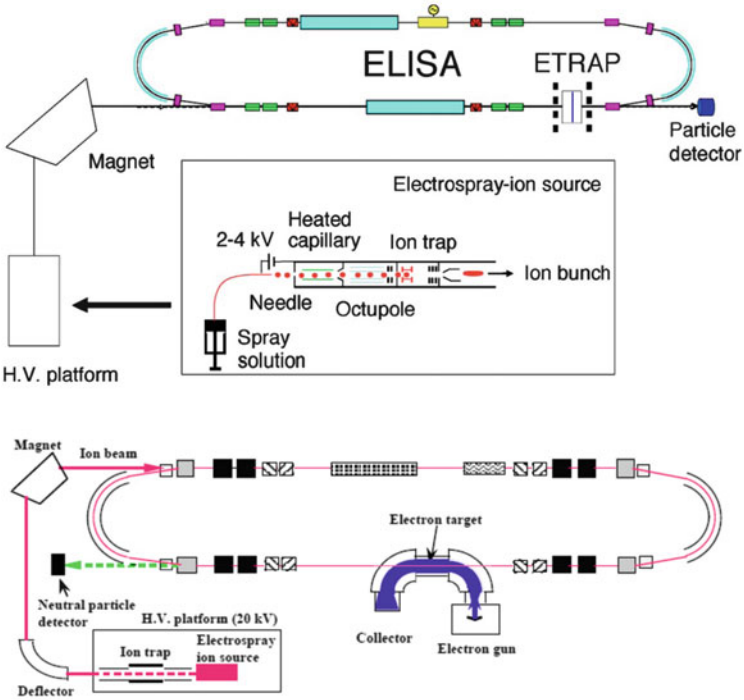

Fig. 4.14 Electrostatic ion storage rings for electron scattering experiments. In the Aarhus set-up (ELISA, *top*) ions cross a beam of electrons that are guided by a magnetic field. Neutral products are detected by a detector positioned at the end of the straight section. In the KEK set-up (*bottom*) the ion and electron beams are instead merged. Taken from [48, 51]. Copyright (2004) by The American Physical Society and © Published under CC BY-NC-SA licence in Journal of Physics: Conference Series by IOP Publishing Ltd

merged beams configuration. At high enough relative energies between the two collision partners, electron detachment may occur to produce neutral fragments, or the ions may become electronically excited also leading to dissociation. The interaction between the incoming electron and the anion is much shorter than vibrational or rotational periods, and the detachment process is therefore vertical. The electron must overcome the Coulomb repulsion to cause detachment, which implies that there is an effective threshold two to three times larger than the vertical detachment energy of the anion. For atomic anions, the relation between the threshold energy and the VDE is $E_{th} = 2^{1/4}\ \mathrm{VDE}^{3/4}$ (in atomic units) [52].

The yield of neutral species is measured as a function of relative energy to produce curves like the ones shown for AMP^- and UMP^- in Fig. 4.15 [48]. The cross section has a smooth energy dependence and can be described by a simple classical model introduced by Andersen and co-workers [53] for atomic anions, $\sigma = \sigma_0\ (1 - E_{th}/E_r)$ where σ_0 is a constant. The model assumes the anion to be spherically symmetric and hence has its limitations for molecular anions. As it is

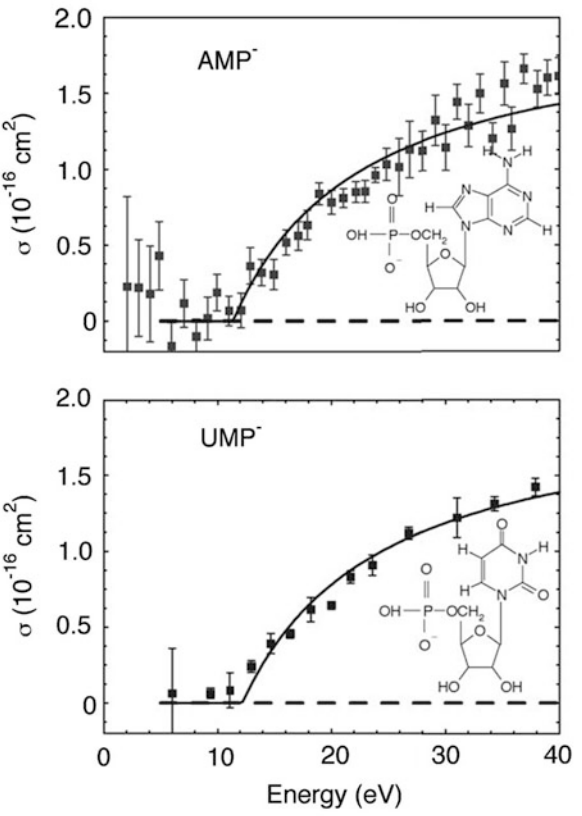

Fig. 4.15 Cross sections for the production of neutral species in interactions between mononucleotide anions and electrons as a function of the electron energy. *Top*: *AMP* adenosine 5′-monophosphate. *Bottom*: *UMP* uridine 5′-monophosphate. The *curves* are based on a simple classical model that only depends on the vertical detachment energy of the anion and the electron energy. Taken from [48]. Copyright (2004) by The American Physical Society

evident from the figure, curves based on this model can be reasonably well fit to the data. The larger polarisability of molecular anions compared to atomic ones implies, however, that the threshold is at higher energies than that predicted from the equation above. In other words, the electrons of the molecular anion avoid the incoming electron by relocating themselves in the electric field set up by the incoming electron, and as a result more energetic incoming electrons are needed to induce detachment [54]. This is seen for the mononucleotides where the measured threshold energy is 12 ± 1 eV while the predicted value based on the equation above is about 10 eV (VDE = 6.05 eV for dAMP [55]).

Resonances are sometimes superimposed on the simple detachment curve and are signatures of the population of short-lived dianion states [56]. The electron tunnels through the Coulomb barrier with a higher probability if there happens to be a state at the kinetic energy of the electron. The dianion lives for a very short time (femtoseconds) before it breaks apart, thus higher cross sections for neutral production are seen. Such resonances were, however, not identified for the two mononucleotides.

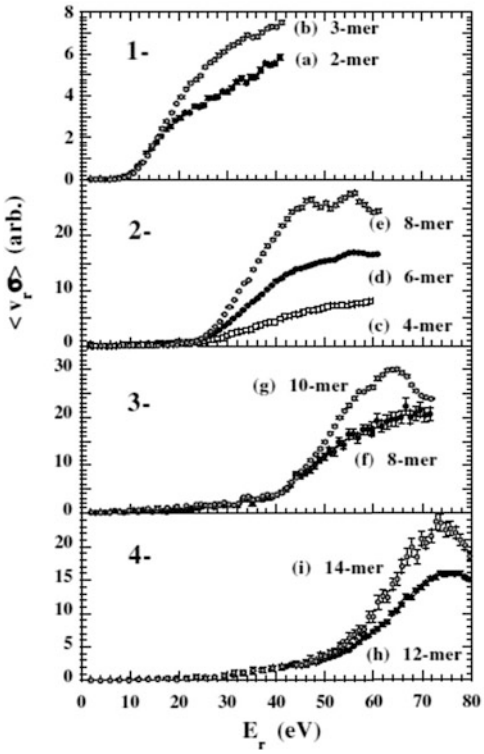

Fig. 4.16 Production rates of neutral species formed after interactions between oligonucleotide anions and electrons as a function of the electron energy. The charge states of the *x*-mers are given on the figure, where *x* is the number of nucleotides. Sequences are (a) d(TG), (b) d(ATG), (c) d(ATGC), (d) d(ATGCTG), (e), (f) d(ATGCATGC), (g) d(ATGCATGCTG), (h) d(ATGCATGCATGC), (i) d(ATGCATGCATGCAT). Taken from [57]. Copyright (2004) by The American Physical Society

Tanabe and co-workers [57] studied oligonucleotide anions, both singly and multiply charged, up to four negative charges and reported production rates of neutral species as a function of electron energy (Fig. 4.16). They found that the threshold for electron detachment increased in steps of about 10 eV starting from about 10 eV for the singly charged ion. The thresholds seen for the monoanions are similar to those measured for the mononucleotide anions described above. The authors explained their findings based on the collective excitation of all valence electrons of the bases and the sugar-phosphate backbone (plasmon state), and this excitation energy was calculated to be about 10 eV somewhat dependent on the length of the oligomer. The authors noted that the experimental threshold energies approximately agree with the 10 eV excitation energy multiplied by the charge state, which implies that the electron would excite a larger number of plasmon quanta the higher the charge state. Further support for this idea was not given.

It is, however, clear that the larger the charge state of an anion, the more difficult it is for the electron to approach and penetrate the repulsive Coulomb barrier, and higher electron energy is therefore needed to cause excitation or electron detachment. Brøndsted Nielsen, Andersen and co-workers [58] also did electron scattering experiments on doubly charged anions, $Pt(CN)_4^{2-}$ and $Pt(CN)_6^{2-}$, and found that the threshold is simply shifted up by a factor equal to the square root of the charge state (i.e. $2^{1/2}$) compared to that of corresponding monoanions. This does not seem

to be enough by itself to explain the increase in threshold with charge state for the oligonucleotide anions.

The storage-ring experiments did not provide information on the dissociation channels after electron detachment or excitation. Mass spectrometric identification of the product ions formed after electron detachment dissociation (EDD) experiments on multiply charged oligonucleotide anions was done by Håkansson and co-workers [42, 43] using a FTICR instrument. They found that more information on the sequence of nucleobases is obtained from such experiments than from collision-induced dissociation due to cleavages of the phosphodiester backbone with no preceding base loss. Complete sequencing is achieved and has enhanced sensitivity compared to ECD of oligonucleotide cations under similar conditions. There is no apparent nucleobase effect, and as direct detachment occurs, it is therefore likely from the deprotonated phosphate backbone. This contrasts with photodetachment experiments, which are described below. Electron photodetachment followed by collision-induced dissociation (EPD) also provides good sequence coverage [59]. Similar to ECD, EDD and EPD may disrupt covalent bonds and preserve non-covalent ones in the dissociation of duplexes containing two non-covalently bound strands.

Work by McLuckey and co-workers [60, 61] suggests that odd-electron oligonucleotide anions gives less base loss than even-electron species under similar activation conditions. However, the fragmentation behaviour may depend on how the radical anions are produced (ETD, EDD, photodetachment or collisional electron detachment [62]) due to differences in whether the electron is detached from the backbone or from the nucleobase [61].

4.4 Photoelectron Spectroscopy

Wang and co-workers [55] reported the first photoelectron spectra of singly charged DNA nucleotide anions (Fig. 4.17). The spectra of $dAMP^-$, $dCMP^-$ and $dTMP^-$ are similar: They have a spectral onset at about 5.4 eV with broad and continuous spectral features. The spectrum of $dGMP^-$ on the other hand displays a weak and well separated band at much lower binding energies while the spectrum at higher energies is similar to those of $dAMP^-$ and $dCMP^-$. Mononucleotides of adenine, thymine and cytosine have electron binding energies slightly above 5 eV while that of $[dGMP–H]^-$ is 0.7 eV lower. Likewise, di- and trinucleotides containing guanine had lower electron binding energies than other strands. The HOMO is therefore on the guanine base (π orbital) and not on the phosphate group. In contrast, it was concluded that electron detachment takes place from the phosphate group for the other three mononucleotides. Dinucleotides and trinucleotides were found to have higher adiabatic detachment energies than mononucleotides. The work clearly established that guanine has the lowest ionisation energy in oligonucleotides, and therefore that guanine would serve as the oxidation site in DNA damage.

Weber et al. [63] did photoelectron spectroscopy experiments on multiply charged oligonucleotide anions $(dB_5)^{4-}$ (deprotonated four times), where B = A

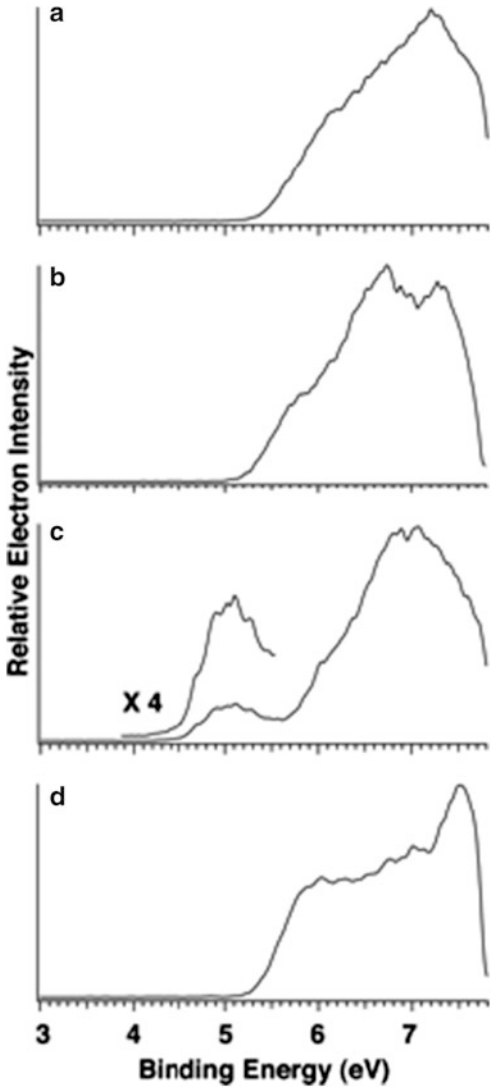

Fig. 4.17 Photoelectron spectra of deprotonated 2′-deoxy-5′-deoxymononucleotide anions at 157 nm (7.866 eV). (**a**) $dAMP^-$, (**b**) $dCMP^-$, (**c**) $dGMP^-$ and (**d**) $dTMP^-$ (*d*). Taken from [55]. Copyright (2004) National Academy of Sciences, USA

or T, and they observed that the adenine strand was much less stable with respect to electron loss than the thymine one. $(dA_5)^{4-}$ actually has a negative electron binding energy, and its existence is due only to the repulsive Coulomb barrier that prevents immediate electron loss.

In recent exciting work, Vonderach et al. [64, 65] have developed a new instrument that allows for conformer-selective photoelectron spectroscopy by combining an electrospray ionisation source, an ion mobility cell, a quadrupole mass filter and a magnetic bottle time-of-flight photoelectron spectrometer. In the case of highly negatively charged oligonucleotides, their work provided evidence for two

classes of structures: one where the excess electrons are localised at the deprotonated phosphate backbone sites and the other where there is at least one deprotonated base in addition to several deprotonated phosphate groups. Ions belonging to the latter class were shown to have the lowest electron binding energy ascribed to the deprotonated base.

4.5 Gas-Phase Absorption Spectroscopy

Absorption spectroscopy of isolated mononucleotide anions in vacuo has been done by Weber and co-workers [66], and similar experiments on oligonucleotide anions were done by Brøndsted Nielsen [67], Gabelica [59, 68, 69] and their co-workers. As an example the spectra of the dAMP mononucleotide and (dA_4) oligonucleotide anions are shown in Fig. 4.18. These were obtained from the yields of photofragment ions in the case of dAMP and photoneutrals in the case of $(dA)_4$ as a function of excitation wavelength. The spectral shapes are quite similar, but the monomer displays an absorption band with maximum at 253 nm while that of the oligomer is slightly blueshifted (by 3 nm) to 250 nm. Such a blueshift has been predicted by theory and is ascribed to the electronic coupling between stacked adenine bases [71]. Thus, the electronic coupling of two bases leads to two new excited state wavefunctions (exciton states) that have energies that are shifted up and down by the same amount relative to the excited state of an isolated monomer. According to theory, the higher exciton state has a larger oscillator strength compared to the lower one, explaining the blueshifted absorption. Excitation to such states may be involved in the DR of oligonucleotide cations as discussed earlier, demonstrating a link between photoexcitation and electron bombardment experiments.

It is also noteworthy that the two gas-phase absorption bands are shifted towards the blue by about 10 nm compared to the recorded spectra of the ions dissolved in water. A similar shift has been observed for the adenine base itself [72], and the shift is therefore not linked to screening of the negative charges in bulk water.

Gabelica and co-workers [59, 66, 67] studied larger multiply charged DNA strands and obtained absorption spectra based on electron photodetachment cross sections, that is, they recorded the yield of the product ion with one less electron as a function of excitation wavelength. Their work indicated that the base is the site of detachment. Guanine has the lowest ionisation energy of the bases, and indeed, guanine strands were found to have the highest electron detachment yields. Theoretical calculations on dinucleotide monophosphates show that the HOMO is located on the base not only for guanine but also for adenine, cytosine and thymine [66]. Hence base excitation triggers electron detachment, clearly demonstrating a link between absorption and electron detachment. Interestingly, the authors also found that internal conversion (IC) could compete with electron detachment, which was evidenced from the formation of fragment ions that are typically formed from vibrationally excited ions. Brøndsted Nielsen and co-workers [67] also demonstrated ultrafast IC even for singly charged strands where the photon energy

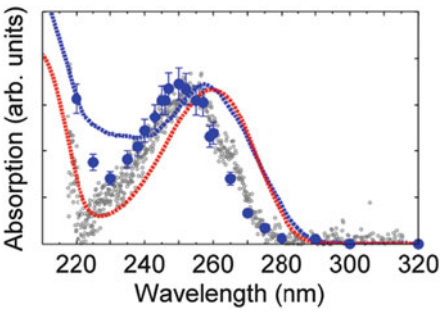

Fig. 4.18 Absorption spectra of $(dA)_4$ and dAMP in vacuo and in aqueous solution. *Blue circles*: $(dA)_4$ anions in vacuo [67]. *Grey points*: dAMP anions in vacuo [66]. *Blue curve*: $(dA)_4$ in solution. *Red curve*: dAMP in solution. Each spectrum is normalised to the band maximum at ca. 250 nm (gas phase) and ca. 260 nm (solution phase). Reproduced from [70] with permission from The Royal Society of Chemistry

was higher than the electron binding energy; hence, it seems important to establish the competition between electron detachment and IC as a function of excitation energy as the absorption spectrum based on electron detachment would be skewed if this ratio changes with wavelength.

In other work also based on electron photodetachment, Rosu et al. [69] found that duplexes and quadruplexes displayed redshifted absorption bands compared to the corresponding single strands, and such spectroscopy could therefore be useful to obtain information on folding motifs.

4.6 Conclusion and Outlook

The study of DNA/RNA ions, isolated in vacuo, and their interactions with electrons and photons has been a very active research area in the last 10 years. Detailed information at the molecular level has been obtained on, e.g. base dehydrogenation and the origin of the lost hydrogen, electron binding energies, absorption band maxima and the electronic coupling between two or more bases in the excited state. The role of hydration was investigated for the formation of dehydrogenated mononucleotide dianions and for the dipole-bound-to-covalent-state transition in nucleobase anions. The field has taken advantage of the development of new advanced instrumental set-ups such as electrostatic ion storage rings that were used by physicists and chemists in collaborative work. Threshold electron energies needed for electron detachment of singly and multiply charged anions were measured in electron scattering experiments, while dissociative recombination experiments on cations revealed a high formation of neutral species at certain electron energies (resonances). Advances in mass spectrometry and electron-induced dissociation methods have shown that nucleic acid sequencing is best achieved by the formation of radical species that undergo breakages of phosphodiester bonds. These methods also hold great promise for the elucidation of conformational structures as non-covalent bonds can be preserved while covalent

ones are broken. More work in the future on partially hydrated nucleic acid ions would be interesting to bridge the physics of bare ions with that of solvated ones and thereby increase the relevance to the biophysical situation. Further studies on the importance of counter ions would be useful to better mimic the real biological environment. Finally, the link between geometric structure and electronic structure is one that deserves much more exploration.

4.7 Summary of Key Concepts

General Concepts
- The Repulsive Coulomb Barrier prevents direct electron attachment to anions.
- Electron attachment or electron detachment results in radical-driven fragmentation.
- Electronic structure is linked to the folding motif.
- Instrumental set-ups used are mass spectrometers, electrostatic storage rings and ion mobility spectrometers.

Concepts Specific to Nucleic Acids
- Electrons induce damage to nucleotide ions.
- Electron attachment to nucleobases causes dehydrogenation.
- Solvation of bare ions results in spectral shifts in the absorption.
- Microhydration and counter ions play roles on electron attachment and/or detachment.
- Photoelectron spectroscopy provides information on electron binding energies and location of highest occupied molecular orbital.
- There are differences in the absorption between single bases, single strands, duplexes and quadruplexes isolated in vacuo.

References

1. Clark LB (1995) Transition moments of 2'-deoxyadenosine. J Phys Chem 99:4466–4470
2. Matsuoka Y, Nordén B (1982) Linear dichroism studies of nucleic acid bases in stretched poly (vinyl alcohol) film. Molecular orientation and electronic transition moment directions. J Phys Chem 86:1378–1386
3. Petke JD, Maggiora GM, Christoffersen REJ (1990) Am Chem Soc 112:5452–5460
4. Wulff DL (1963) Kinetics of thymine photodimerization in DNA. Biophys J 3:355–362
5. Lamola AA, Eisinger J (1968) On the mechanism of thymine photodimerization. Proc Natl Acad Sci USA 59:46–51
6. Johns HE, Pearson ML, Helleiner CW, Leblanc JC (1964) The ultraviolet photochemistry of thymidylyl-(3′→5′)-thymidine. J Mol Biol 9:503–524
7. Crespo-Hernandez CE, Cohen B, Hare PM, Kohler B (2004) Ultrafast excited-state dynamics in nucleic acids. Chem Rev 104:1977–2019

8. Middleton CT, de La Harpe K, Su C, Law YK, Crespo-Hernández CE, Kohler B (2009) DNA excited-state dynamics: from single bases to the double helix. Annu Rev Phys Chem 60:217–239
9. Kohler B (2010) Nonradiative decay mechanisms in DNA model systems. J Phys Chem Lett 1:2047–2053
10. Brøndsted Nielsen S, Andersen JU, Forster JS, Hvelplund P, Liu B, Pedersen UV, Tomita S (2003) Photodestruction of adenosine 5′-monophosphate (AMP) nucleotide ions *in vacuo*: statistical versus nonstatistical processes. Phys Rev Lett 91:048302
11. Markovitsi D, Gustavsson T, Banyasz A (2010) Absorption of UV radiation by DNA: spatial and temporal features. Mutat Res 704:21–28
12. Markovitsi D (2009) Interaction of UV radiation with DNA helices. Pure Appl Chem 81:1635–1644
13. Markovitsi D, Gustavsson T, Vayá I (2010) Fluorescence of DNA duplexes: from model helices to natural DNA. J Phys Chem Lett 1:3271–3276
14. Cobut V, Frongillo Y, Patau JP, Goulet T, Fraser M-J, Jay-Gerin JP (1998) Monte Carlo simulation of fast electron and proton tracks in liquid water – I. Physical and physicochemical aspects. Radiat Phys Chem 51:229–243
15. LaVerne JA, Pimblott SM (1995) Electron-energy loss distributions in solid, dry DNA. Radiat Res 141:208–215
16. Boudaïffa B, Cloutier P, Hunting D, Huels MA, Sanche L (2000) Resonant formation of DNA strand breaks by low-energy (3 to 20 eV) Electrons. Science 287:1658–1660
17. Martin F, Burrow PD, Cai Z, Hunting D, Sanche L (2004) DNA strand breaks induced by 0-4 eV electrons: the role of shape resonances. Phys Rev Lett 93:068101
18. Desfrancois C, Abdoul-Carime H, Schermann JP (1996) Electron attachment to isolated nucleic acid bases. J Chem Phys 104:7792–7794
19. Gohlke S, Abdoul-Carime H, Illenberger E (2003) Dehydrogenation of adenine induced by slow (<3eV) electrons. Chem Phys Lett 380:595
20. Hanel G, Gstir B, Scheier P, Probst M, Farizon B, Farizon M, Illenberger E, Märk TD (2003) Electron attachment to uracil: effective destruction at subexcitation energies. Phys Rev Lett 90:188104
21. Denifl S, Ptasinska S, Cingel M, Matejcik S, Scheier P, Märk TD (2003) Electron attachment to the DNA bases thymine and cytosine. Chem Phys Lett 377:74–80
22. Denifl S, Ptasinska S, Probst M, Hrusak J, Scheier P, Märk TD (2004) Electron attachment to the gas-phase DNA bases cytosine and thymine. J Phys Chem A 108:6562–6569
23. Ptasinska S, Denifl S, Scheier P, Illenberger E, Märk TD (2005) Bond- and site-selective loss of H atoms from nucleobases by very-low-energy electrons (<3eV). Angew Chem Int Ed 44:6941–6943
24. Abdoul-Carime H, Gohlke S, Illenberger E (2004) Site-specific dissociation of DNA bases by slow electrons at early stages of irradiation. Phys Rev Lett 92:168103
25. Théodore M, Sobczyk M, Simons J (2006) Cleavage of thymine N_3-H bonds by low-energy electrons attached to base π^* orbitals. Chem Phys 329:139–147
26. Anusiewicz I, Berdys J, Sobczyk M, Skurski P, Simons J (2004) Effects of base π-stacking on damage to DNA by low-energy electrons. J Phys Chem A 108:11381–11387
27. Berdys J, Anusiewicz I, Skurski P, Simons J (2004) Damage to model DNA fragments from very low-energy (<1 eV) electrons. J Am Chem Soc 126:6441–6447
28. Berdys J, Skurski P, Simons J (2004) Damage to model DNA fragments by 0.25-1.0 eV electrons attached to thymine π^* orbital. J Phys Chem B 108:5800–5805
29. Barrios R, Skurski P, Simons J (2002) Mechanism for damage to DNA by low-energy electrons. J Phys Chem B 106:7991–7994
30. Nielsen AB, Hvelplund P, Liu B, Brøndsted Nielsen S, Tomita S (2003) Coulomb explosion upon electron attachment to a four-coordinate monoanionic metal complex. J Am Chem Soc 125:9592–9593

31. Liu B, Hvelplund P, Brøndsted Nielsen S, Tomita S (2004) Formation of C_{60}^{2-} dianions in collisions between C_{60}^{-} and Na atoms. Phys Rev Lett 92:168301
32. Liu B, Tomita S, Rangama J, Hvelplund P, Brøndsted Nielsen S (2003) Electron attachment to "naked" and microsolvated nucleotide anions: detection of long-lived dianions. ChemPhysChem 4:1341–1344
33. Liu B, Hvelplund P, Brøndsted Nielsen S, Tomita S (2004) Hydrogen loss from nucleobase nitrogens upon electron attachment to isolated DNA and RNA nucleotide anions. J Chem Phys 121:4175–4179
34. Ptasińska S, Denifl S, Scheier P, Märk TD (2004) Inelastic electron interaction (attachment/ ionization) with deoxyribose. J Chem Phys 2004(18):8505–8511
35. Liu B, Haag N, Johansson H, Schmidt HT, Cederquist H, Brøndsted Nielsen S, Zettergren H, Hvelplund P, Manil B, Huber BA (2008) Electron capture induced dissociation of nucleotide anions in water nanodroplets. J Chem Phys 128:075102
36. Liu B, Brøndsted Nielsen S, Hvelplund P, Zettergren H, Cederquist H, Manil B, Huber BA (2006) Collision-induced dissociation of hydrated adenosine monophosphate nucleotide ions: protection of the ion in water nanoclusters. Phys Rev Lett 97:133401
37. Hendricks JH, Lyapustina SA, de Clercq HL, Snodgrass JT, Bowen KH (1996) Dipole bound, nucleic acid base anions studied via negative ion photoelectron spectroscopy. J Chem Phys 104:7788–7791
38. Hendricks JH, Lyapustina SA, de Clercq HL, Bowen KH (1998) The dipole bound-to-covalent anion transformation in uracil. J Chem Phys 108:8–11
39. Wyer JA, Cederquist H, Haag N, Huber BA, Hvelplund P, Johansson HAB, Maisonny R, Brøndsted Nielsen S, Rangama J, Rousseau P, Schmidt HT (2009) On the hydrogen loss from protonated nucleobases after electronic excitation or collisional electron capture. Eur J Mass Spectrom 15:681–688
40. Schultz KN, Håkansson K (2004) Rapid electron capture dissociation of mass-selectively accumulated oligodeoxynucleotide dications. Int J Mass Spectrom 234:123–130
41. Håkansson K, Hudgins RR, Marshall AG, O'Hair RAJ (2003) Electron capture dissociation and infrared multiphoton dissociation of oligonucleotide dications. J Am Soc Mass Spectrom 14:23–41
42. Yang J, Håkansson K (2006) Fragmentation of oligonucleotides from gas-phase ion-electron reactions. J Am Soc Mass Spectrom 17:1369–1375
43. Yang J, Mo J, Adamson JT, Håkansson K (2005) Characterization of oligonucleotides by electron detachment dissociation Fourier transform ion cyclotron resonance mass spectrometry. Anal Chem 77:1876–1882
44. Smith SI, Brodbelt JS (2009) Electron transfer dissociation of oligonucleotide cations. Int J Mass Spectrom 283:85–93
45. Wah T, Chan D, Choy MF, Chan WYK, Fung YME (2009) A mechanistic study of the electron capture dissociation of oligonucleotides. J Am Soc Mass Spectrom 20:213–226
46. Tanabe T, Starikov EB, Noda K, Saito M (2006) Resonant neutral-particle emission after collisions of electrons with base-stacked oligonucleotide cations in a storage ring. Chem Phys Lett 430:380–385
47. Tanabe T, Starikov EB, Noda K (2008) Resonant neutral-particle emission correlated with base-base interactions in collisions of electrons with protonated and sodiated dinucleotide monocations. Chem Phys Lett 467:154–158
48. Bluhme H, Jensen MJ, Brøndsted Nielsen S, Pedersen UV, Seiersen K, Svendsen A, Andersen LH (2004) Electron scattering on stored mononucleotide anions. Phys Rev A 70:020701
49. Andersen JU, Hvelplund P, Brøndsted Nielsen S, Tomita S, Wahlgreen H, Møller SP, Pedersen UV, Forster JS, Jørgensen TJD (2002) The combination of an electrospray ion source and an electrostatic storage ring for lifetime and spectroscopy experiments on biomolecules. Rev Sci Instrum 73:1284–1287
50. Tanabe T, Noda K, Syresin E (2004) An electrostatic storage ring with a merging electron beam device at KEK. Nucl Instrum Methods Phys Res A 532:105–110

51. Tanabe T (2007) Neutral-particle emission from multiply charged biomolecular ions in collisions with electrons. J Phys Conf Ser 58:17–24
52. Seiersen K, Bak J, Bluhme H, Jensen MJ, Brøndsted Nielsen S, Andersen LH (2003) Electron-impact detachment of O_3^-, NO_3^- and SO_2^- ions. Phys Chem Chem Phys 5:4814–4820
53. Andersen LH, Mathur D, Schmidt HT, Vejby-Christensen L (1995) Electron-impact detachment of D^-: near-threshold behavior and the nonexistance of D^{2-} resonances. Phys Rev Lett 74:892–895
54. El Ghazaly MOA, Svendsen A, Bluhme H, Brøndsted Nielsen S, Andersen LH (2005) Electron scattering on *p*-benzoquinone anions. Chem Phys Lett 405:278–281
55. Yang X, Wang X-B, Vorpagel ER, Wang L-S (2004) Direct experimental observation of the low ionization potentials of guanine in free oligonucleotides by using photoelectron spectroscopy. Proc Natl Acad Sci USA 101:17588–17592
56. Svendsen A, Bluhme H, El Ghazaly MOA, Seiersen K, Brøndsted Nielsen S, Andersen LH (2005) Tuning the continuum ground state energy of NO_2^{2-} by water molecules. Phys Rev Lett 94:223401
57. Tanabe T, Noda K, Saito M, Starikov EB, Tateno M (2004) Regular threshold-energy increase with charge for neutral-particle emission in collisions of electrons with oligonucleotide anions. Phys Rev Lett 93:043201
58. El Ghazaly MOA, Svendsen A, Bluhme H, Nielsen AB, Brøndsted Nielsen S, Andersen LH (2004) Electron scattering on centrosymmetric molecular dianions $Pt(CN)_4^{2-}$ and $Pt(CN)_6^{2-}$. Phys Rev Lett 93:203201
59. Gabelica V, Tabarin T, Antoine R, Rosu F, Compagnon I, Broyer M, De Pauw E, Dugourd P (2006) Electron photodetachment dissociation of DNA polyanions in a quadrupole ion trap mass spectrometer. Anal Chem 78:6564–6572
60. McLuckey SA, Stephenson JL Jr, O'Hair RAJ (1997) Decompositions of odd- and even-electron anions derived from deoxy-polyadenylates. J Am Soc Mass Spectrom 8:148–154
61. Gao Y, McLuckey SA (2013) Electron transfer followed by collision-induced dissociation (NET-CID) for generating sequence information from backbone-modified oligonucleotide anions. Rapid Commun Mass Spectrom 27:249–257
62. Liu B, Hvelplund P, Brøndsted Nielsen S, Tomita S (2003) Electron loss and dissociation in high energy collisions between multiply charged oligonucleotide anions and noble gases. Int J Mass Spectrom 230:19–24
63. Weber JM, Ioffe IN, Berndt KM, Loffler D, Friedrich J, Ehrler OT, Danell AS, Parks JH, Kappes MM (2004) Photoelectron spectroscopy of isolated multiply negatively charged oligonucleotides. J Am Chem Soc 126:8585–8589
64. Vonderach M, Ehrler OT, Weis P, Kappes MM (2011) Combining ion mobility spectrometry, mass spectrometry, and photoelectron spectroscopy in a high-transmission instrument. Anal Chem 83:1108–1115
65. Vonderach M, Ehrler OT, Matheis K, Weis P, Kappes MM (2012) Isomer-selected photoelectron spectroscopy of isolated DNA oligonucleotides: phosphate and nucleobase deprotonation at high negative charge states. J Am Chem Soc 134:7830–7841
66. Marcum JC, Halevi A, Weber JM (2009) Photodamage to isolated mononucleotides-photodissociation spectra and fragment channels. Phys Chem Chem Phys 11:1740–1751
67. Nielsen LM, Pedersen SØ, Kirketerp M-BS, Brøndsted Nielsen S (2012) Absorption by DNA single strands of adenine isolated *in vacuo*: the role of multiple chromophores. J Chem Phys 136:064302
68. Gabelica V, Rosu F, Tabarin T, Kinet C, Antoine R, Broyer M, De Pauw E, Dugourd P (2007) Base-dependent electron photodetachment from negatively charged DNA strands upon 260-nm laser irradiation. J Am Chem Soc 129:4706–4713
69. Rosu F, Gabelica V, De Pauw E, Antoine R, Broyer M, Dugourd P (2012) UV spectroscopy of DNA duplex and quadruplex structures in the gas phase. J Phys Chem A 116:5383–5391

70. Nielsen LM, Hoffmann SV, Brøndsted Nielsen S (2013) Electronic coupling between photo-excited stacked bases in DNA and RNA strands with emphasis on the bright states initially populated. Photochem Photobiol Sci 12(8):1273–1285
71. Lange AW, Herbert JM (2009) Both intra- and interstrand charge-transfer excited states in aqueous B-DNA are present at energies comparable to, or just above, the (1)pi pi* excitonic bright states. J Am Chem Soc 131:3913–3922
72. Li L, Lubman DM (1987) Ultraviolet visible absorption-spectra of biological molecules in the gas-phase using pulsed laser-induced volatilization enhancement in a diode-array spectrophotometer. Anal Chem 59:2538–2541